ELSEVIER

Ceramics International 32 (2006) 665–671

CERAMICS
INTERNATIONAL

www.elsevier.com/locate/ceramint

The photoluminescence of $SrAl_2O_4$:Sm phosphors

Tzu-Piao Tang *, Chih-Ming Lee, Fu-Cheng Yen

Department of Materials and Mineral Resources Engineering, National Taipei University of Technology, 1, Sec. 3, Chung-Hsiao E., Taipei 106, Taiwan, ROC

Received 21 December 2004; received in revised form 21 February 2005; accepted 22 March 2005
Available online 5 October 2005

Abstract

A red emitting $SrAl_2O_4$:Sm phosphor powder was synthesized by the solid-state method. The phosphor showed Sm^{3+} emission when fired in a reducing atmosphere at 1200 °C. The intraion emission spectra of Sm^{3+} ($^4G_{5/2} \Rightarrow {}^4H_{5/2}$) indicates $Sm^{3+} + h\upsilon \Rightarrow Sm^{2+} + \hbar_{VB}$ reaction to occur with intense emission lines located at 562, 596 and 643 nm. Results indicate that fluxing agents such as LiF and B_2O_3 play an important role in the photoluminescence (PL) emission intensity of $SrAl_2O_4$ powders. Also an increased content of the hexagonal phase in the $SrAl_2O_4$ powder boosts the PL intensity. The emission intensity becomes stronger as the firing temperature increases from 600 to 1200 °C. $SrAl_2O_4$:Sm shows the maximum PL intensity at 10 wt% of B_2O_3 addition. The B_2O_3 addition affects the spacing of the ($\bar{2}$ 1 1) planes but not the (2 2 0) and (2 1 1) planes. This derives from B^{3+} ion replacing the Al^{3+} ion in the ($\bar{2}$ 1 1) plane and causing shrinkage of the crystal lattice, which induces crystal defects and hence produces a stronger PL intensity.

Keywords: Luminescence; Phosphor; Host; $SrAl_2O_4$; Flux; B_2O_3; LiF; Activator; Sm; Emission

1. Introduction

Luminescent materials are used in a variety of applications, which include fluorescent tubes, cathode-ray tubes, X-ray imaging screens, and other emission display devices. Phosphors are generally prepared using an inorganic powder of host material containing 1–5 mol% activator ions and 1–10 wt% fluxing agents [1,2]. Among the various phosphors, $SrAl_2O_4$ has excellent properties such as high brightness, no radiation, safety, long duration, and environmental capability. It has two structures, a high-temperature hexagonal phase (β-phase) and a low-temperature monoclinic phase (α-phase). Host materials of $Sr_3Al_2O_6$, $SrAl_2O_4$, $SrAl_4O_7$, $SrAl_{12}O_{19}$ were prepared by controlling the molar ratio of SrO and Al_2O_3 powders in several studies [3,4]. With Eu and Dy doping of the host materials, the photoluminescence intensity and afterglow property of $SrAl_2O_4$ were improved [5]. Though the effects of Eu and Dy co-dopant on $SrAl_2O_4$ phosphors have been reported [6–8], rare information regarding the role of Sm in phosphors is shown in the literature. Also, it is important to clarify the effects of the B_2O_3 flux on the crystal defects of the $SrAl_2O_4$:Sm phosphors. In this study, Sm is doped into the $SrAl_2O_4$ phosphors by solid-state reaction. The effects of flux agents such as LiF and B_2O_3, Sm concentration, and firing conditions on the photoluminescence were investigated. A luminescence mechanism associated with the $SrAl_2O_4$ powders was proposed based on the $SrAl_2O_4$ powders morphology and the photoluminescence. The effects of B_2O_3 addition on the structure and luminescence were investigated. The luminescence mechanism of this system is presented through the results of the crystal structure and the photoluminescence behavior of the $SrAl_2O_4$ powders.

2. Experimental

The $SrAl_2O_4$ powder was prepared from SrO and Al_2O_3 powders with Al/Sr ratio of 2/1, according to the reaction $SrO + Al_2O_3 \Leftrightarrow SrAl_2O_4$. Small amount (≈5 wt%) of fluxing agents such as B_2O_3 and LiF were added in each

---

* Corresponding author. Tel.: +886 2 27712171; fax: +886 2 27317185.
E-mail address: tptang@ntut.edu.tw (T.-P. Tang).

0272-8842/$30.00 © 2005 Elsevier Ltd and Techna Group S.r.l. All rights reserved.
doi:10.1016/j.ceramint.2005.03.034

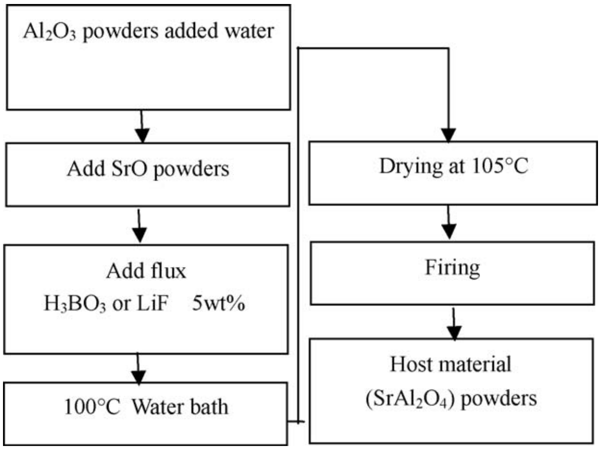

Fig. 1. Flow chart of the preparation of $SrAl_2O_4$ phosphor powders by solid-state reaction.

sample [2]. The processing flow chart for the nominal compositions is shown in Fig. 1. After sintering at 1200 °C for 1 h in air, the $SrAl_2O_4$ compound was blended with $Sm(NO_3)_3{\cdot}6H_2O$, with the molar ratio of 0.2, 0.5, 1.0, 1.2, 1.3, 1.4, 1.5, 1.7, and 2.0%. Then LiCl was used as a flux during the subsequent heat treatment in a reducing atmosphere at 1200 °C for 1 h. The process flow is shown in Fig. 2. $SrAl_2O_4$:Sm phosphors were prepared using SrO and Al_2O_3 powders through the reaction of $SrO + Al_2O_3 \Leftrightarrow SrAl_2O_4$. The atomic ratio of Al/Sr must be precisely controlled to be 2/1. 0, 2.5, 5, 7.5, 10, 12.5 wt% B_2O_3 and 2.5 wt% Sm activator were added to the powders, which were then fired at 1300 °C in an inert atmosphere for 1 h and cooled in air. Emission spectra were measured by a Shimadzu spectrofluorophotometer (RF-5301), with a standard lamp. The excitation spectra were obtained by scanning wavelength from 220 to 450 nm monitored at 650 nm. The emission wavelength was scanned from 545 to 745 nm, excited at 405 nm. X-ray diffraction (XRD) was used to confirm the structure of the products, using a Rigaku D/Max B with Cu Kα_1 radiation at 40 kV and 15 mA and a scanning rate of 4° (2θ)/min.

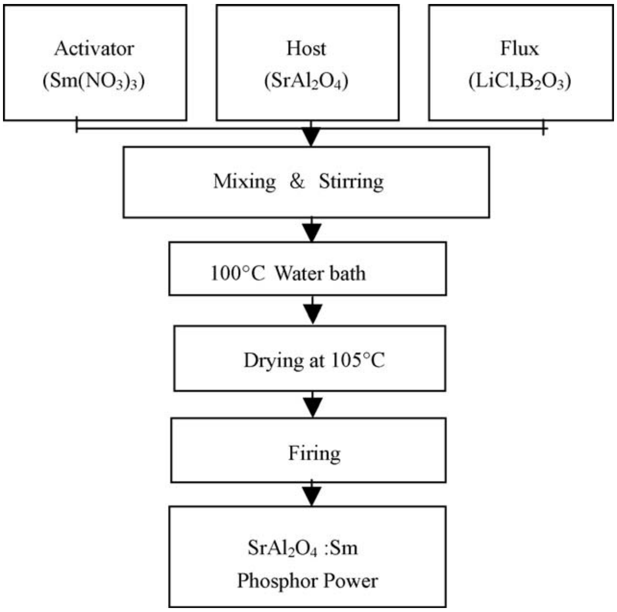

Fig. 2. Flow chart of the preparation of Sm doped $SrAl_2O_4$ phosphor powders.

3. Result and discussion

Fig. 3 shows the X-ray diffraction patterns of the as-prepared powder after heat treatment (Fig. 1). It is apparent that a good crystalline $SrAl_2O_4$ powder could be obtained at the soaking temperature of about 1200 °C, which is 500 °C lower than for the conventional solid-state reaction method. The XRD pattern of the as-prepared compound well matches with the monoclinic phase, though minor impurities can be observed in the phase analysis. The results are consistent with the ones reported in the literature [3]. The transition temperature for the high-temperature hexagonal $SrAl_2O_4$ phase (β-phase) to the low-temperature monoclinic phase (α-phase) occurs at 650 °C [9].

To study the effect of the Sm concentration on the crystallization of $SrAl_2O_4$:Sm powders, it is essential that the processing conditions should be kept constant while

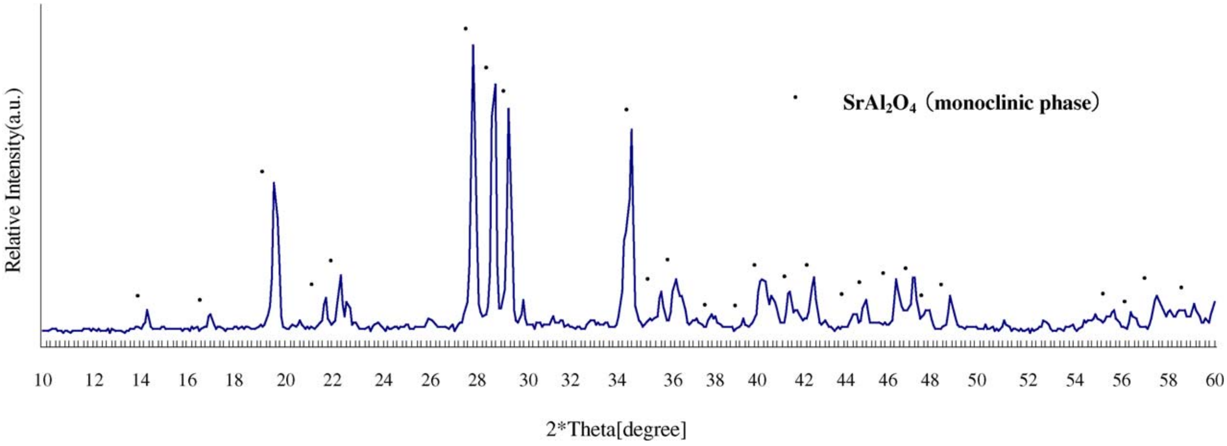

Fig. 3. X-ray spectra of $SrAl_2O_4$ powder with 5 wt% B_2O_3 fired in air at 1200 °C for 1 h.

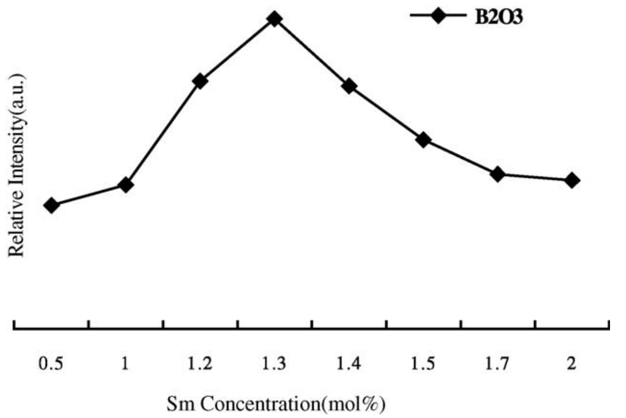

Fig. 4. Emission spectrum of $SrAl_2O_4$:Sm phosphor with various amount of Sm and fired at 1200 °C in reductive atmosphere (compared at peak 596 nm).

varying the Sm concentration. Therefore, a series of nine samples with different Sm concentration ranging from 0.2 to 2.0 mol% were prepared simultaneously under the same reaction conditions. Figs. 4 and 5 show the intensity and PL spectra for the $SrAl_2O_4$ phosphor powders with different amounts of Sm additions. The peak intensity strongly depends on Sm concentration. The intensity of the Sm^{3+} characteristic emission peak increases with increasing the amount of the Sm dopant up to 1.3 mol%, then the luminescence intensity begins to quench as the Sm content continues to increase.

The firing temperature is another important parameter that affects the grain size and thus the Sm^{3+} PL emission of $SrAl_2O_4$:Sm phosphors. As expected, an increase in grain size with the firing temperature was observed. In addition, the PL spectra of the $SrAl_2O_4$:Sm powders show the Sm^{3+} emission to increase significantly with increasing firing temperature from 600 to 1200 °C, as indicated in Figs. 6 and 7. It is apparent that the Sm^{3+} emission efficiency is very sensitive to the firing temperature. Both the grain size increases and the Sm^{3+} emission intensity increases by firing at a higher temperature.

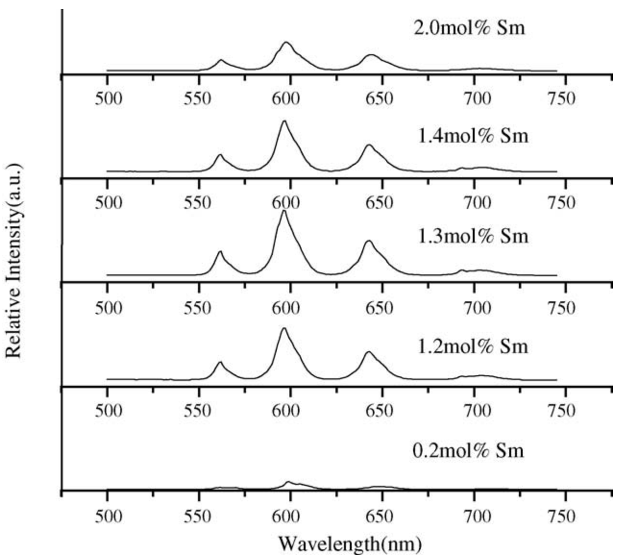

Fig. 5. PL spectra of $SrAl_2O_4$:Sm red phosphor with various Sm concentrations.

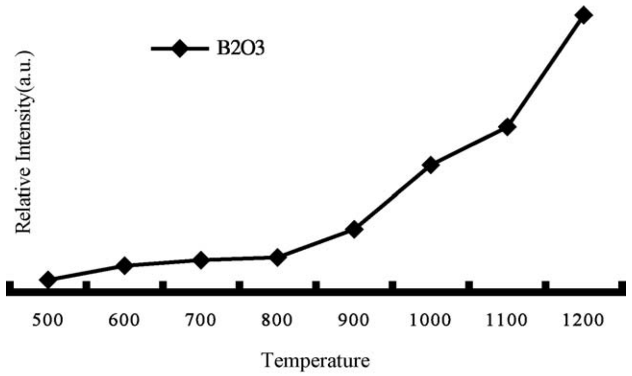

Fig. 6. Emission spectrum of $SrAl_2O_4$:Sm phosphor prepared at various firing temperatures (compared at peak 596 nm).

The $SrAl_2O_4$:Sm phosphor has three main Sm^{3+} emission peaks at 562, 596, and 643 nm, which are located in the orange-red region. The emission spectra is contributed from the intra-4f orbital transition from the $4G_{5/2}$, level to the $^6H_{5/2}$, $^6H_{7/2}$ and $^6H_{9/2}$ levels of Sm^{3+}, as shown in Fig. 8. The strongest emission ($^4G_{5/2} \Rightarrow {}^4H_{7/2}$) is located at 596 nm, and the others are 562 and 643 nm. Particularly, lines at 596 and 643 nm are the most important emissions, which are located in the red-orange color range. They are produced by the electron transition, which is attributed to the intra-4f orbital transition. The Sm^{3+} acted as a trap level which captured the free holes in the $SrAl_2O_4$:Sm phosphor system. The trapped and detrapped recombination procedure brought about the brightness [10].

Fig. 8 shows the effect of the fluxing agents on the emission intensity, and Fig. 9 shown the PL spectra of the

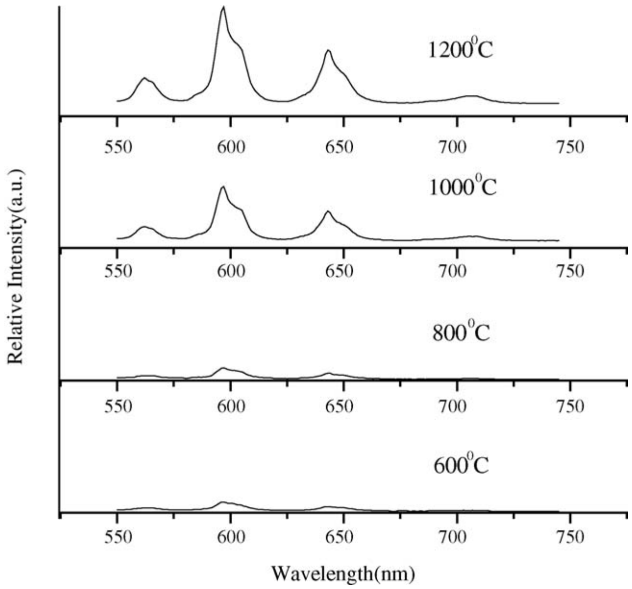

Fig. 7. The spectra intensity of $SrAl_2O_4$:Sm powders prepared at firing temperatures of 600, 800, 1000 and 1200 °C.

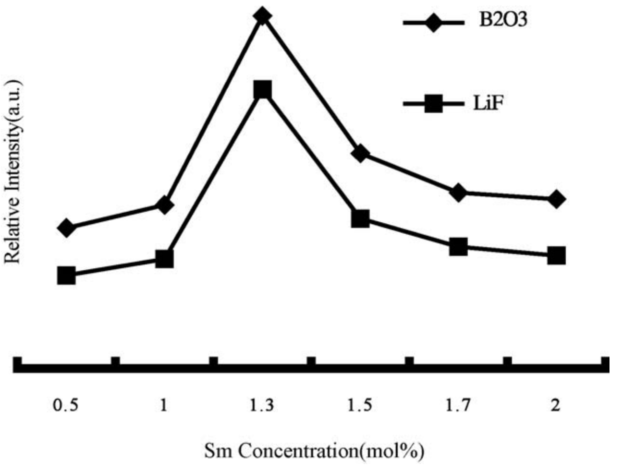

Fig. 8. The effect of the fluxing agents in the emission intensity (compared at peak 596 nm).

$SrAl_2O_4$:Sm (1.3 mol%) with different fluxes and fired at 1200 °C in a reducing atmosphere. The addition of B_2O_3 or LiF can reduce the synthesis temperature of $SrAl_2O_4$ because it can provide a liquid medium and increase the diffusion rate, as observed in the literature [11,12]. However, B_2O_3 has a great advantage over LiF as it yields a higher PL intensity. B ions can replace the Al ions in the tetrahedral sites of the structure and result in the lattice distortions, due to its low ionic radius (B^{3+}: 23 pm) compared to the Al ion (Al^{3+}: 57 pm). The maximum emission intensity was obtained at the B_2O_3 content of 5 wt%.

The effect of B_2O_3 concentration on the luminescence characteristic of $SrAl_2O_4$:Sm phosphors is shown in Fig. 10. The peak intensity varies with B_2O_3 concentration. Sm-doped $SrAl_2O_4$ powder excited by an ultraviolet light exhibits three sharp peaks which were contributed from the intra-4f orbital transition from the $^4G_{5/2}$ level to the $^6H_{5/2}$, $^6H_{7/2}$ and $^6H_{9/2}$ levels [13]. The intensity of the Sm^{3+} characteristic emission peak increases at increasing the amounts of B_2O_3 up to 10 wt% and then levels off.

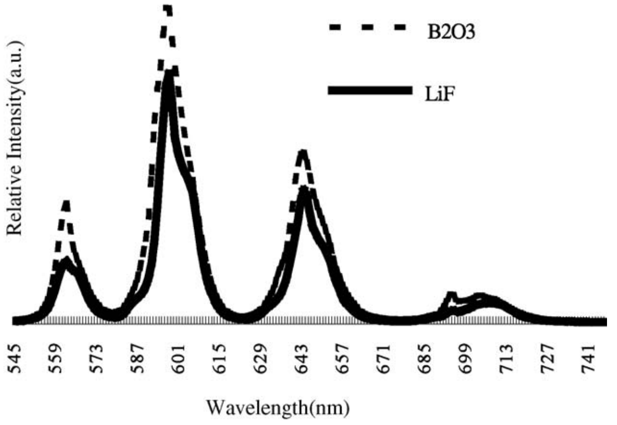

Fig. 9. PL spectra of $SrAl_2O_4$:Sm (1.3 mol%) with different fluxes and fired at 1200 °C in reductive atmosphere.

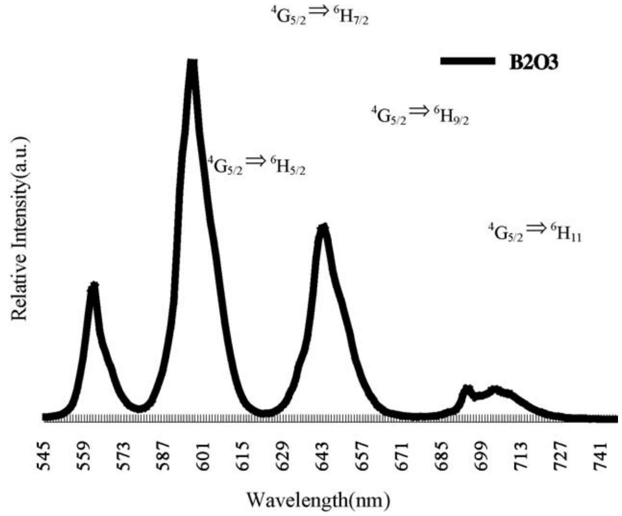

Fig. 10. PL spectrum of $SrAl_2O_4$:Sm (1.3 mol%) powder fired at 1200 °C in reducing atmosphere.

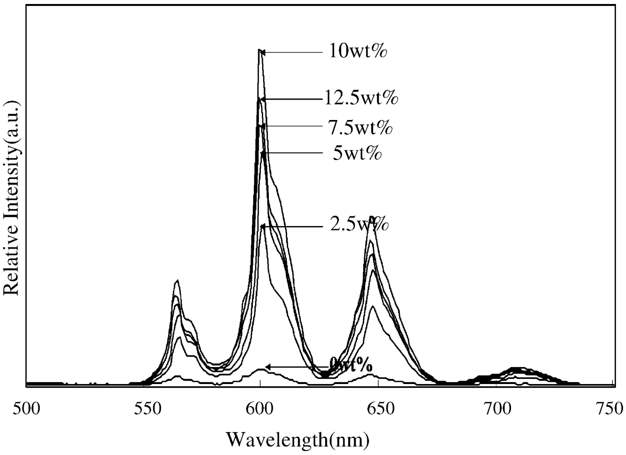

Fig. 11. The effect of B_2O_3 concentration on the emission intensity of $SrAl_2O_4$:Sm phosphor (Sm = 2.0 wt%).

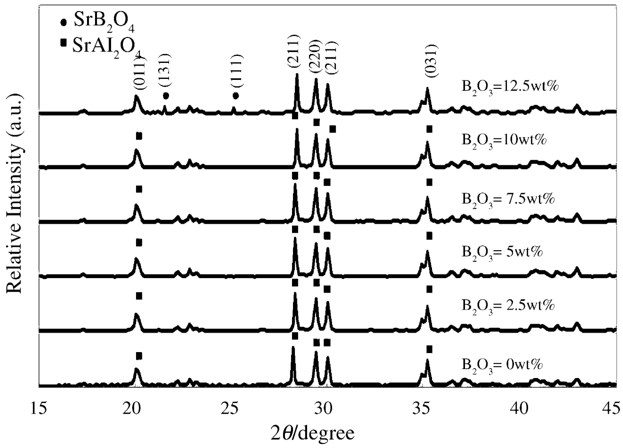

Fig. 12. X-ray spectra of $SrAl_2O_4$:Sm powders with various B_2O_3 concentration (Sm = 2.0 wt%).

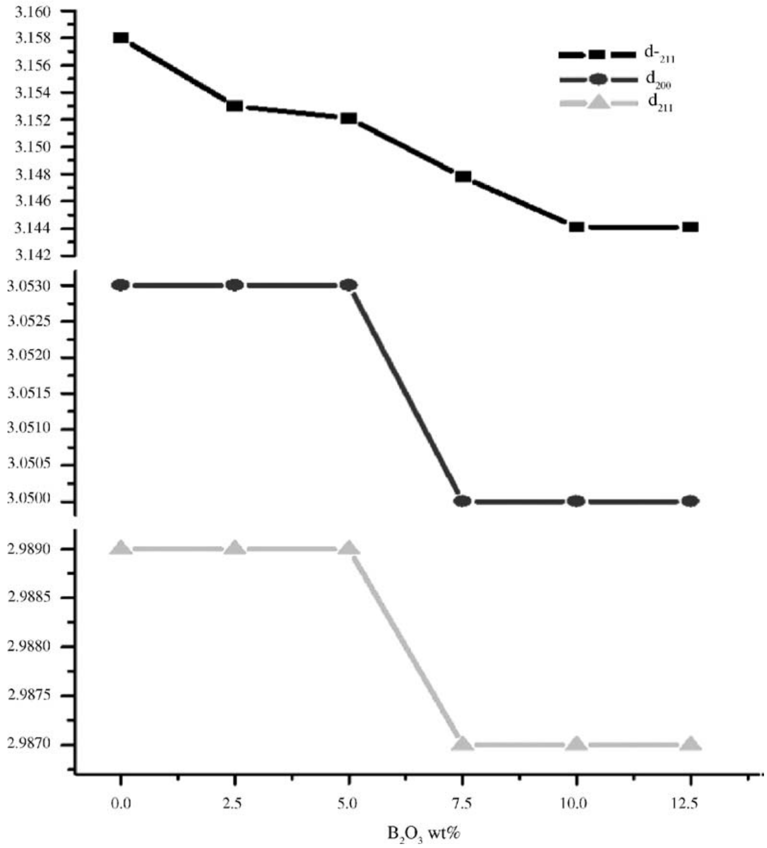

Fig. 13. Effect of inter-planar spacing with various concentration of B_2O_3 in $SrAl_2O_4$:Sm phosphors (Sm = 2.0 wt%).

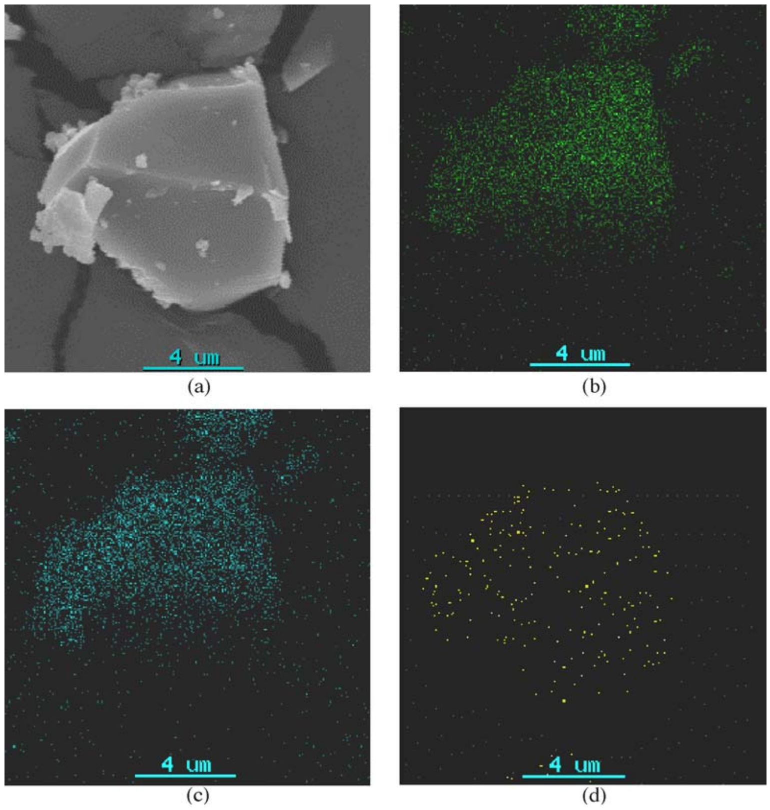

(a) (b)

(c) (d)

Fig. 14. X-ray mapping pictures of $SrAl_2O_4$:Sm phosphor (B_2O_3 = 5 wt%). (a) Secondary electron image (b) Al (c) Sr (d) Sm.

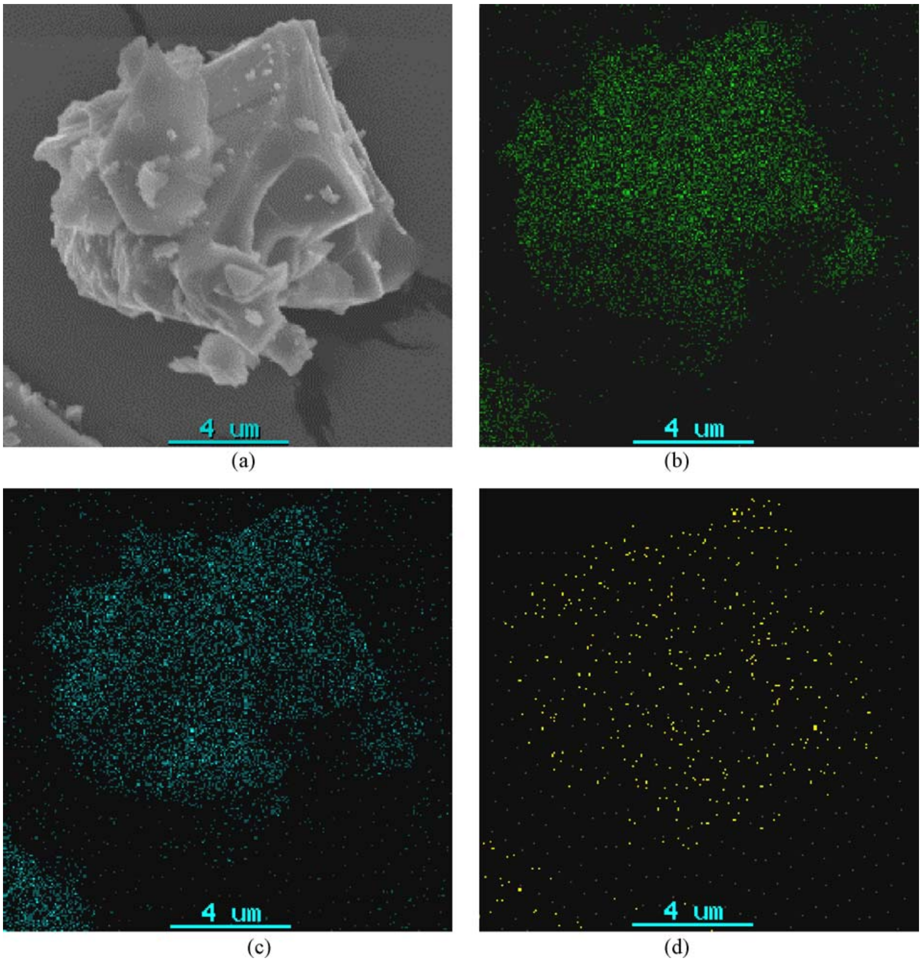
(a) (b) (c) (d)

Fig. 15. X-ray mapping pictures of $SrAl_2O_4$:Sm phosphor (B_2O_3 = 10 wt%). (a) Secondary electron image (b) Al (c) Sr (d) Sm.

The influence of B_2O_3 concentration on crystal structure of $SrAl_2O_4$:Sm phosphors is shown in Fig. 11. The addition of B_2O_3 provides a liquid medium and increases the diffusion rate during firing. The crystal structure of $SrAl_2O_4$:Sm phosphors remains as pure phase when the B_2O_3 concentration increases. As the concentration of B_2O_3 reaches 12.5 wt%, a second SrB_2O_4 phase is found, which is consistent with the observation of the luminescence characteristics of $SrAl_2O_4$:Sm powders.

From the XRD results in Fig. 12, the inter-planar spacing of $(\bar{2}\,1\,1)$, (2 2 0) and (2 1 1) planes were calculated. The influence of various concentrations of B_2O_3 agents on the inter-planar spacing of the host material is presented in Fig. 13. They show that as the concentration of B_2O_3 increases from 0 to 12.5 wt%, the inter-planar spacing of $(\bar{2}\,1\,1)$ reduces from 3.158 to 3.144 Å, the inter-planar spacing of (2 2 0) decreases from 3.053 to 3.050 Å, and the inter-planar spacing of (2 1 1) decreases from 2.989 to 2.987 Å. The contraction of $(\bar{2}\,1\,1)$ planes produces $SrAl_2O_4$ crystal lattice shrinkage and thus enhances the PL intensity.

Figs. 14 and 15 show energy dispersive spectroscopy x-ray mapping of $SrAl_2O_4$:Sm powder with 5 wt% B_2O_3 and 10 wt% B_2O_3, respectively. The results indicate that the Sm element uniformly distributed on the powder surface. It is apparent that the uniformity of Sm activator on the surfaces of $SrAl_2O_4$:Sm powder with 10 wt% B_2O_3 addition is better than for 5 wt% B_2O_3 addition, and thus generates a stronger PL intensity. Up to 10 wt% of B_2O_3 addition can yield a superior phosphor, which is due to the fact that the $SrAl_2O_4$ crystal structure has suitable shrinkage as well as the Sm can uniformly distribute on the surfaces. Hence, B_2O_3 addition on $SrAl_2O_4$:Sm phosphors has a stronger PL intensity.

4. Conclusions

(1) $SrAl_2O_4$:Sm phosphor, prepared by solid-state reaction, shows three main emission peaks at 562, 596 and 643 nm.
(2) Samples of phosphor powders prepared with 0.2, 0.5, 1.0, 1.2, 1.3, 1.4, 1.5, 1.7, 2.0 mol% Sm additions show fluorescence intensity to increase with the activator concentration (Sm) up to 1.3 mol% and then begin to decrease.
(3) The firing temperature plays an important role in $SrAl_2O_4$:Sm powders. The emission intensity increases as the firing temperature increased from 600 to 1200 °C.

(4) The introduction of B_2O_3 dopant in the $SrAl_2O_4$:Sm powders appears to yield crystal defects that can trap the holes generated by the excitation of Sm ions. Results in this study show that the performance of $SrAl_2O_4$:Sm powders is significantly enhanced by adding 5 wt% of B_2O_3 as a flux. The fluorescence intensity increases by increasing the concentration of the B_2O_3 flux up to 10 wt% and then begins to decrease. Best emission was obtained by 10 wt% B_2O_3 addition.

(5) The spacing of $(\bar{2}\,1\,1)$ planes reduces significantly as the B^{3+} replaces the Al^{3+} ion sites in the $SrAl_2O_4$ crystal lattice, which caused the shrinkage of crystal structure. This induces a higher number of crystal defects and hence a stronger PL intensity.

Acknowledgements

The authors appreciated the financial support provided by National Science Council Taiwan, ROC; under contract whose number is NSC-90-2216-E-027-012. The authors also indebted to Winbond Electronics Corp. for equipment support.

References

[1] A. Jestin Lenus, K. Govinda Rajan, M. Yousuf, D. Sornadurai, B. Purniah, Mater. Lett. 54 (2002) 70–74.

[2] Y.-T. Yu, B.-G. Kim, J.-M. Yoon, J. Mining Mater. Processing Inst. Japan 115 (1999) 705–708.

[3] Z. Misirli, H. Erkalfa, O.T. Ozkan, Ceram. Int. 22 (1996) 33–37.

[4] T. Katsumata, K. Sasajima, T. Nabae, S. Komuro, T. Morikawa, J. Am. Ceram. Soc. 81 (2) (1998) 413–416.

[5] T. Katsumata, T. Nabae, K. Sasajima, S. Komuro, T. Morikawa, J. Electrochem. Soc. 144 (September (9)) (1997) 243–245.

[6] M. Kamada, J. Murakami, N. Ohno, J. Lumin. 87–89 (2000) 1042–1044.

[7] H. Jorma, H. Jungner, M. Lastusaai, J. Niittykoski, J. Alloys Compd. 323–324 (2001) 326–330.

[8] D. Wang, Q. Yin, Y. Li, M. Wang, J. Lumin. 97 (April (1)) (2002) 1–6.

[9] S. Ito, S. Bangno, K. Suzuki, Z. Physik. Chem. Neue. Folge 105 (1977) 173.

[10] K. Swiatek, M. Godlewski, Phys. Rev. B 43 (12) (1991) 9956–9957.

[11] M. Marchal, E. Cordoncillo, P. Scribano, M. Vallet-Regi, J.B. Carda, paper, 1999, pp. 1–2.

[12] I.C. Chen, Ph.D. Thesis, National Chiao Tung University, Shin Chu, 2000, pp. 65–73.

[13] T.P. Tang, M.R. yang, K.S. Chen, Ceram. Int. 26 (2000) 153–155.